Acta Applicandae Mathematicae **38:** 149–161, 1995.

The Ubiquitous Ellipse

GUILLERMO SAPIRO[1]* and ALFRED M. BRUCKSTEIN[2]
[1]*Department of Electrical Engineering,*
[2]*Department of Computer Science, Technion–Israel Institute of Technology, Haifa 32000, Israel*

(Received: 22 March 1993; in final form: 16 February 1994)

Abstract. We discuss three different affine invariant evolution processes for smoothing planar curves. The first one is derived from a *geometric heat-type flow*, both the initial and the smoothed curves being differentiable. The second smoothing process is obtained from a discretization of this affine heat equation. In this case, the curves are represented by planar *polygons*. The third process is based on *B-spline* approximations. For this process, the initial curve is a planar polygon, and the smoothed curves are differentiable and even analytic. We show that, in the limit, all three affine invariant smoothing processes collapse any initial curve into an *elliptic point*.

Mathematics Subject Classifications (1991). 35Q80, 41A15, 52B99, 53A15.

Key words: affine invariant, multi-scale smoothing, geometric heat flows, polygons, B-splines, ellipses.

1. Introduction

Multiscale descriptions of signals have been the subject of extensive research. A possible formalism for this topic comes from the idea of multiscale filtering that was introduced by Witkin [44], and developed in a variety of frameworks over the past decade [5, 24, 27, 30, 46]. The idea of scale-space (multiscale) filtering is very simple and can be formulated as follows: Given an initial signal $\Phi_0(\mathbf{X})$: $\mathbb{R}^n \to \mathbb{R}^m$, the scale-space is obtained by filtering it with a kernel $\mathcal{K}(\mathbf{X}, t)$: $\mathbb{R}^n \to \mathbb{R}^m$, where $t \in \mathbb{R}^+$ represents the scale. In other words, the scale-space representation of $\Phi_0(\mathbf{X})$ is defined as

$$\Phi(\mathbf{X}, t) := \Omega_{\mathcal{K}(\mathbf{X},t)}\left[\Phi_0(\mathbf{X})\right], \tag{1}$$

where $\Omega_{\mathcal{K}(\cdot,t)}[\cdot]$ represents the action of the filter $\mathcal{K}(\cdot, t)$. Larger values of t correspond to signals at coarser resolutions.

A classical example of a scale-space kernel is the Gaussian one. In this case, the scale-space is linear, and the filter in (1) is defined via convolution. The Gaussian kernel is one of the most studied in the theory of scale-spaces [5, 24, 27, 46]. It has some very interesting properties, one of them being the signal Φ obtained from it is the solution of the heat equation (with Φ_0 as initial condition) given by

$$\frac{\partial \Phi}{\partial t} = \Delta \Phi.$$

One of the lessons from the Gaussian example, is that the scale-space can be obtained as the solution of a partial differential *evolution equation*. The idea of connecting multi-scale representations to evolution equations was developed in [1–2, 3, 25, 26, 37] with a view to various applications.

* Current address: LIDS, MIT, Cambridge, MA 02139, U.S.A.

We shall consider 'time' varying closed planar curves $\mathcal{C}(u,t)$: $[a,b] \times [0,\tau) \to \mathbb{R}^2$. Note that from the point of view of image analysis, a simple closed planar curve is the boundary of a planar shape, and a time-varying planar curve describes an evolving shape. We describe three different affine invariant [16] multiscale representations of planar curves, representations that give increasingly smooth curves. The first one is derived from a *geometric heat-type flow* [35–37], where both the initial and the smoothed curves are differentiable (smooth). We should note, however, that this theory can be extended to nonsmooth initial curves using the theory of viscosity solutions as in [2] or the novel result for Lipschitz curves in [4]. The second one is obtain from a discretization of this affine heat equation [11]. In this case, the curves are represented by *polygons*. The third process is based on *B-spline* approximations [33]. For this process, the initial curve is given by a polygon, and the smoothed curves are differentiable and analytic. As a nice consequence of affine invariance, we show that all these processes shrink an arbitrary initial curve into an *elliptic point*, i.e., a curve that when normalized in order to enclose a given strictly positive area, it approaches an ellipse of the same area.

This paper is organized as follows: Section 2 presents the affine geometric heat flow. The discrete analogue of this flow is given in Section 3. The B-spline based multiscale representation is described in Section 4. A short discussion and concluding remarks are found in Section 5.

2. The Affine Geometric Heat Flow

Consider a family of parameterized planar curves* $\mathcal{C}(u,t)$: $[a,b] \times [0,\tau) \to \mathbb{R}^2$, defined via the evolution equation

$$\frac{\partial \mathcal{C}}{\partial t} = \frac{\partial^2 \mathcal{C}}{\partial p^2}, \qquad \mathcal{C}(u,0) = \mathcal{C}_0(u). \tag{2}$$

If $p \equiv u$, then (2) becomes the classical heat equation discussed in the Introduction. If, however, $p \equiv v$, where v is the *Euclidean arc-length* [43], the *Euclidean shortening flow*, or *Euclidean geometric heat flow*, is obtained [21, 23]. Gage and Hamilton [21] proved that any simple convex curve converges into a circular point when evolving according to the Euclidean geometric flow. Then Grayson [23] proved that any simple nonconvex curve converges into a convex one. Therefore, any simple curve evolves into a circular point when evolving according to the Euclidean geometric heat flow. This flow defines a geometric Euclidean invariant multiscale representation [2, 26].

A natural question that arises is whether one can obtain a multiscale representation, similar to that obtained via the Euclidean heat flow, invariant under the group of affine transformations. In [35, 36], it was shown that if $p \equiv s$ in (2), where s is the *affine arc-length*, i.e., the basic affine invariant parameterization given by [8, 10, 35]

$$s(u) \triangleq \int_{u_0}^{u} \left(\frac{\partial \mathcal{C}(\xi)}{\partial \xi} \times \frac{\partial^2 \mathcal{C}(\xi)}{\partial \xi^2} \right)^{1/3} \mathrm{d}\xi,$$

then the *affine shortening flow*, or *affine geometric heat flow*, is obtained. The main results of [35] are:

* We assume that the curves are sufficiently smooth, such that the derivatives are well defined.

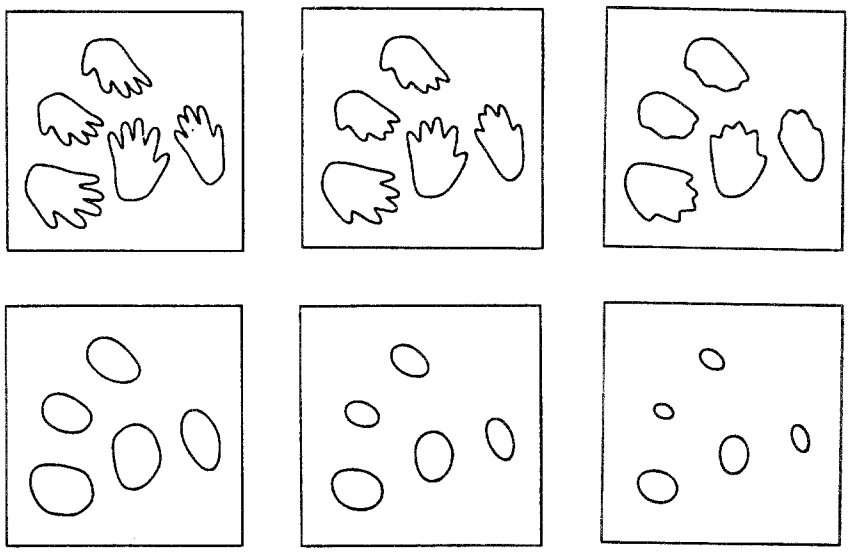

Fig. 1. Example of the affine geometric heat flow. The *hands* are related by affine transformations.

THEOREM 1. *If $C(\cdot,0)$ is convex, then it remains convex when the curve evolves according to* (2), *$p \equiv s$, and the solution of this evolution equation exists as long as the area enclosed by the evolving curve is bounded away from zero.*

THEOREM 2. *Any convex, smooth, and embedded curve, converges to an elliptical point when evolving according to* (2), *with $p \equiv s$. The convergence is in the sense that the normalized dilated curves converge in the Hausdorff metric to an ellipse.*

These results were also extended for nonconvex curves. Since C_{ss} is not defined at inflection points [8, 35], this involves the study of the following flow [36]:

$$\frac{\partial C}{\partial t} = \begin{cases} C_{ss} & \text{noninflection point,} \\ 0 & \text{inflection point.} \end{cases} \tag{3}$$

Equation (3) is the natural extension of (2) (with $p \equiv s$), and for this flow, the following results holds [4, 36, 38]:

THEOREM 3. *Let $C(\cdot,0)$: $S^1 \to \mathbb{R}^2$ be a smooth embedded curve in the plane. Then there exists a family C: $S^1 \times [0,T) \to \mathbb{R}^2$ satisfying* (3), *such that $C(\cdot,t)$ is smooth and embedded for all $t < T$ and, moreover, there is a $t_0 < T$ such that for all $t > t_0$, $C(\cdot,t)$ is smooth and convex.*

Therefore, by the results in [4, 35, 36, 38], any simple smooth curve converges to an elliptic point (becoming convex first) when evolving according to the affine geometric heat flow, being (3) the affine invariant analogue of the Euclidean heat flow.

The affine flow (3) can be implemented using an efficient numerical algorithm for curve evolution proposed by Sethian and Osher in [31], and based on this, a geometric affine invariant multiscale representation for planar curves is available [37]. It is important to note that a curve evolving according to this flow, gets smoother in the sense that the total curvature decreases [37]. Figure 1 presents an example of outlines of a *hand*, related by affine transformations, evolving according to (3).

3. Polygonal Affine Invariant Evolution

Consider a planar polygon P with N vertices. P may be nonconvex and even self-intersecting. Each one of the vertices P_i of P, $i = 0, 1, \ldots, N-1$, can be represented by a point in the complex plane, i.e., the polygon P is an N-dimensional vector over the complex plane, $P = [P_0, P_1, \ldots, P_{N-1}]^T$.

A general linear evolution of the polygon is described by

$$P(n) = MP(n-1), \qquad P(0) = P, \tag{4}$$

where M is a constant $N \times N$ complex matrix, and $n \in \mathbb{N}^+$ is the discrete time. In the evolution described by Equation (4), the new coordinates of each vertex are obtained by a linear combination (with possible complex weights) of the coordinates of the previous polygon. The number of vertices is constant in the evolution process.

The linear polygonal evolution given by Equation (4), is affine invariant if M is real, i.e., if the points of $P(n)$ and $\widetilde{P}(n)$ are related by an affine mapping, and $P(n)$ evolves according to (4), $\widetilde{P}(n)$ also evolves according to (4) with the same evolution matrix M.

Next, we shall show that a polygonal version of the *affine heat flow* (3) takes the form of (4). (For details, and general results on linear polygonal evolutions, see [11].) We set the parameterization p of the polygon P to be consecutive integers (modulo N) at the vertices, so that for $i \in \{0, 1, \ldots, N-1\}$, $P(i, n) \equiv P_i(n)$ (the ith vertex of the polygon $P(n)$). Note that since polygon vertices (i.e., curve breakpoints) are affine invariant, a straightforward discrete affine arc-length may be chosen so that at the ith vertex is arc-length i. With this, naturally affine invariant parameterization, a straightforward discretization of (3) leads to the following evolution equation for the polygon vertices:

$$P(i, n+1) = (1-c)P(i, n) + \frac{c}{2}P(i-1, n) + \frac{c}{2}P(i+1, n). \tag{5}$$

This equation implies a linear evolution of type (4), where M is a real circulant matrix with first row m given by

$$m = \left[1 - c, \frac{c}{2}, 0, \ldots, 0, \frac{c}{2}\right]. \tag{6}$$

The geometric interpretation of this transformation readily follows from the observation that as c increases from 0 to $\frac{2}{3}$, the point $P_i(n)$ moves from its previous position, $P_i(n-1)$, to the local center of mass of the points P_i, P_{i-1}, P_{i+1} at time $(n-1)$. Therefore, the evolution of each polygon vertex is a step towards the local weighted center of mass.

A well-known property of circulant matrices [22] is that they can be represented as

$$M = U \Lambda U^{-1}, \tag{7}$$

where U is an orthogonal matrix such that its i-column, $i = 0, 1, \ldots, N-1$, is given by

$$W_i = \left[w^0, w^i, w^{2i}, \ldots, w^{i(N-1)}\right]^T, \quad w = \exp\left\{j\,\frac{2\pi}{N}\right\}, \; j = \sqrt{-1}.$$

$\Lambda = \text{diag}\{\lambda_1, \lambda_2, \ldots, \lambda_N\}$, and λ_i is the ith eigenvalue of M given by

$$\lambda_i = N \cdot IDFT_i(m^T) = mW_i.$$

Here, $IDFT_i(\cdot)$ stands for the ith element of the Inverse Discrete Fourier Transform. It is easy to check that $U^{-1} = (1/NU)^*$ (where U^* stands for the conjugate transpose of U) [22].

Now, from (4) and (7), we obtain

$$\begin{aligned} P(n) &= M^n P = \frac{1}{N} U \Lambda^n U^* P = \frac{1}{N} \sum_{i=0}^{N-1} (\lambda_i)^n W_i (W_i)^* P \\ &= \frac{1}{N} \sum_{i=0}^{N-1} (\lambda_i)^n DFT_i(P) W_i. \end{aligned}$$

Assume that the matrix M in (4) is normalized such that $\max_i |\lambda_i| = 1$, and define

$$P^\infty(n) \triangleq \frac{1}{N} \sum_{\{i:\ |\lambda_i|=1\}} \exp\{jn \arg(\lambda_i)\} DFT_i(P) W_i, \tag{8}$$

where $\arg(x)$ stands for the complex argument of x. We clearly have that $P(n)$ converges to $P^\infty(n)$ in the sense that

$$\lim_{n\to\infty} \left|P_i(n) - P_i^\infty(n)\right| = 0 \quad \text{for } i = 0, 1, \ldots, N-1.$$

In the case of m as in (6) (i.e., the discretized affine heat flow), it is easy to show that λ_i is real for all i. Also, λ_0, the biggest eigenvalue, is $\lambda_0 = 1$. Therefore,

$$P^\infty(n) = P^\infty = \left(\frac{1}{N} \sum_{i=0}^{N-1} P_i\right) [1, 1, \ldots, 1]^T, \tag{9}$$

i.e., P^∞ is simply the centroid of the initial polygon. Since the limiting polygon P^∞ is a point, we can ask about the shape $P(n)$ takes while approaching P^∞. In order to investigate this, consider the polygon $P(n) - P^\infty$ normalized as follows:

$$B(n) \triangleq \frac{1}{N(\max_{i\neq 0}\{|\lambda_i|\})^n} \sum_{i\neq 0} (\lambda_i)^n DFT_i(P) W_i.$$

Define

$$B^\infty(n) \triangleq \frac{1}{N} \sum_{\{i:\ |\lambda_i| = \max_{i\neq 0}\{|\lambda_i|\}\}} \exp\{jn \arg(\lambda_i)\} DFT_i(P) W_i, \tag{10}$$

and $B^\infty(n)$ provides the geometric behavior of the polygon when $n \to \infty$ (i.e., when $P(n)$ converges to P^∞). From Equation (10), it is clear that the shape of the polygon, when approaching P^∞, is governed by the second greatest eigenvalues.

A polygon Q will be called a *poly-ellipse* if all its points are located on an ellipse, and Q has no self-intersections. Hence, a poly-ellipse is a natural polygonal approximation of an ellipse. For the evolution defined by (4), together with (6), we have the following result [11]:

THEOREM 4. *Let $P(n)$ be a polygon evolving according to the evolution Equation* (6), *with $P(0) = P$. If*

(1) $N \neq 4$ *and* $0 \leqslant c \leqslant \frac{2}{3}$,
(2) $DFT_1(P) \neq 0$ *or* $DFT_{N-1}(P) \neq 0$,

then $P(n)$ converges to the centroid of the initial polygon, and the normalized polygon $B^\infty(n)$ converges to a fixed poly-ellipse.

Proof (*Outline*). First of all, for m as in Equation (6), we already saw that the polygon converges to the centroid (Equation (9)). It is easy to prove that for this M, the second greatest eigenvalues are obtained for $i = 1$ and $i = N - 1$, i.e.,

$$|\lambda_1| = |\lambda_{N-1}| > |\lambda_i| \quad (\forall i \neq 0, 1, N-1).$$

From Equation (10), we have

$$B^\infty(n) = \frac{1}{N}\left(DFT_1(P)W_1 + DFT_{N-1}(P)W_{-1}\right),$$

showing that B^∞ is a poly-ellipse of the form

$$R\left[\alpha\cos(2\pi i/N), \beta\sin(2\pi i/N)\right]^T + V,$$

where α and β are constants, R is a rotation matrix, and V is a translation vector. Hence not only is B^∞ a poly-ellipse but also it is an affine transformation of a regular polygon. □

Note that B^∞ is independent of the selection of the parameter c (as long as $c \in [0, \frac{2}{3}]$). This parameter simply controls the speed of convergence.

The result in Theorem 4 is not unexpected in the light of the observation that this evolution is a discretized polygonal version of the affine curve evolution studied in [36]. It is also interesting to note that while the discrete analog is so simple to analyze, the study of the continuous affine geometric heat flow requires advanced methods from the theory of partial differential equations and affine differential geometry. Figure 2 shows examples of this polygon evolution.

We end this section by pointing out that after we studied this subject of the discrete version of the affine geometric heat flow, we learned that the topic of linear polygonal evolutions has an extensive literature devoted to it, starting from a beautiful paper by Darboux written in 1878 [15]. He considered the problem of polygon evolution described by a slightly different rule:

Considérons un polygone plan ou gauche de n côtés $A_1, A_2, \ldots, A_n$. On forme un second polygone de même nombre de côtés en joignant les milicux $A'_1, A'_2, \ldots, A'_n$ does côtés $A_1A_2, \ldots, A_nA_1$ du premier. De ce deuxième polygone on déduit un troisième par la même loi, puis un quatrième, et, en continuant indéfiniment, on obtain ainsi une suite illimitée de polygones. Je me propose de démontrer que ces polygones deviennent

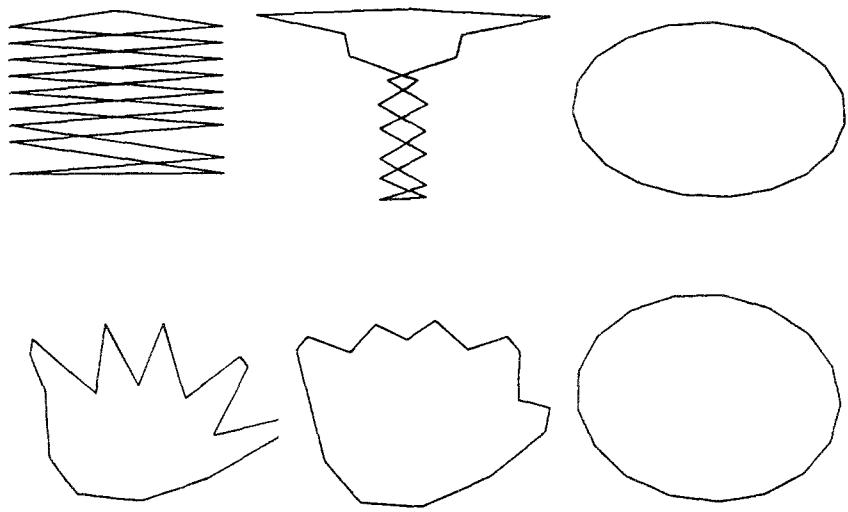

Fig. 2. Two examples of the discrete (polygonal) model of the affine invariant evolution.

de plus en plus petits, c'est-à-dire que tous les sommets du polygons de rang n de la série précédente se rapprochent d'un point fixe quand n croit indéfiniment; et, en même temps, je déterminerai la forme de ce polygone quand il devient infiniment petit...

Subsequently, long after the results by Darboux were forgotten, other researchers rediscovered some of these results. Among them, we mention I. J. Schoenberg in 1950 [39], J. H. Cadwell in 1953 [12], E. R. Berlekamp *et al.* in 1965 [7], L. Fejes Tóth in 1969 [20]. Many other researchers worked on this and related fascinating problems connecting Fourier analysis with basic geometry [9, 13, 14, 19, 28, 29, 42, 45].

4. The B-Spline Based Representation

We shall discuss next yet another affine smoothing process. Note that in the first example, the curves are continuous, and in the second one, they are represented by planar polygons. In the smoothing process presented below, the original curve is a polygon, while the evolved smoothed curves are continuous.

We briefly review the theory of B-spline approximations. For details, see [6, 17].

Let $C(u)$: $[a, b] \to \mathbb{R}^2$ be a planar curve with Cartesian coordinates $[x(u), y(u)]$. Polynomials are computationally efficient to work with, but it is not always possible to describe well enough a curve C using single polynomials for x and y. Therefore, in applications, the curve is described as a sequence of segments, each one defined by a given polynomial. The segments are joined together to form a *piecewise polynomial* curve. The joints between the polynomial segments occur at special curve points called *knots*. The sequence $u_1, u_2, \ldots$ of knots is required to be nondecreasing. The 'distance' between two consecutive knots can be constant or not. Two successive polynomial segments are

joined together at a given knot u_j in such a way that the resulting piecewise polynomial has d continuous derivatives. Of course, the order of the polynomials depends on d.

Formally, the curve C is a *B-spline* approximation of the series of points $V_i = [x_i, y_i]$, $1 \leqslant i \leqslant N$, called *control vertices*, if it can be written as

$$C_k(u) = \sum_{i=1}^{N} V_i B_{i,k}(u), \tag{11}$$

where $B_{i,k}(\cdot) = B(\cdot; u_i, u_{i+1}, \ldots, u_{i+k})$ is the ith *B-spline basis* of order k for the knot sequence $[u_1, \ldots, u_{N+k}]$. In particular, $B_{i,k}$ is a piecewise polynomial function of degree $< k$, with breakpoints $u_j, \ldots, u_{j+k}$.

The B-spline basis $B_{i,k}$ can be computed using a recursive formula of the following form [6, 17, 18]:

$$B_{i,1}(u) = \begin{cases} 1, & u_i \leqslant u \leqslant u_{i+1}, \\ 0, & \text{otherwise}, \end{cases}$$

$$B_{i,k}(u) = \frac{u - u_i}{u_{i+k-1} - u_i} B_{i,k-1} + \frac{u_{i+k} - u}{u_{i+k} - u_{i+1}} B_{i+1,k-1}.$$

Several properties can be proven for this basis $B_{i,k}$:

(1) $B_{i,k}(u) \geqslant 0$.

(2) $B_{i,k}(u) \equiv 0$ outside the interval $[u_i, u_{i+k}]$. This property shows the locality of the approximation: Moving a given control vertex affects only a well defined portion of the curve.

(3) The basis is normalized:

$$\sum_i B_{i,k}(u) = 1 \quad \text{on } [u_k \ldots u_{N+1}].$$

The multiplicity of the knots governs the smoothness. If a given number τ occurs r times in the knot sequence $[u_i, \ldots, u_{i+k}]$, then the first $k - r - 1$ derivatives of $B_{j,k}$ are continuous at the breakpoint τ.

Observe that from (11), the affine invariant property of the B-spline representation is immediate. If $\{\widetilde{V}_i\}_1^N$ is obtained from $\{V_i\}_1^N$ by an affine transformation (A, T) (A being a real 2×2 matrix and $T \in \mathbb{R}^2$ a translation vector), i.e.,

$$\{V_i\}_1^N = \{A\widetilde{V}_i + T\}_1^N,$$

then

$$\widetilde{C}_k(u) = AC_k(u) + T, \tag{12}$$

where

$$C_k(u) = \sum_{i=1}^{N} V_i B_{i,k}(u), \qquad \widetilde{C}_k(u) = \sum_{i=1}^{N} \widetilde{V}_i B_{i,k}(u).$$

Based on this, we can define a B-spline based, affine invariant, multiscale shape representation (*BAIM*) of the polygon described by the points $\{V_i\}_i^N$, as the family of

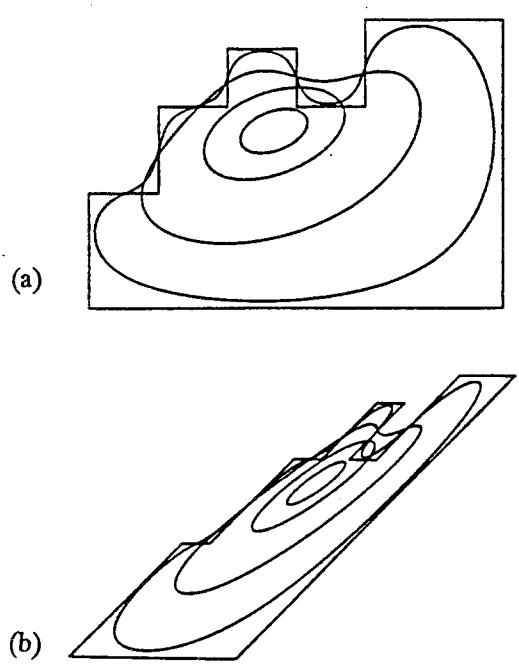

Fig. 3. An example of the *BAIM* and its affine invariant property. (a) A 12 points polygon and its correspondent B-spline representations or order $k = 2^i$, $i = 1, 2, 4, 6, 7$. Note the convergence to the centroid, with an elliptical shape. (b) The original polygon is obtained via an affine transformation of the one in Figure 3. The corresponding *BAIM* s related to the one in Figure 3a by the same transformation.

curves C_k obtained from (11) for $k = 2, 3, \ldots$ [33]. Note that in contrast with the multi-scale representations described in Section 2, the *BAIM* is discrete in the scale parameter $(k = 2, 3, \ldots)$. This representation was recently extended in [34] to obtain a continuous in scale representation. The extension is based on using subdivision schemes for defining B-spline basis in C^r, $r \in [0, \infty)$.

Figure 3* presents the first *BAIM* example (see also [32]). The polygon contains 12 points. In Figure 3a, the initial polygon is given, together with the corresponding *BAIM* for $k = 2^i$, $i = 1, 2, 4, 6, 7$. In Figure 3b, the initial polygon is obtained via an affine transformation of the polygon in Figure 3a. Due to the affine invariant property, the corresponding *BAIM* is related to the one in Figure 3a by the same affine transformation.

The following theorem shows the behavior of the B-spline approximations as the order k increases (see Figure 3).

THEOREM 5. *As k increases $(k \to \infty)$, the B-spline representation converges to the centroid of the control points $\{V_i\}_1^N$, its shape becoming elliptical.*

Proof (Outline). Let's represent the control points as complex numbers, i.e., $V_i = [x_i + jy_i]$. Then, using the Fourier series expansion of the basis functions $B_{i,k}(u)$ [40, 41],

* The examples here presented were implemented using the Matlab Spline Toolbox [18].

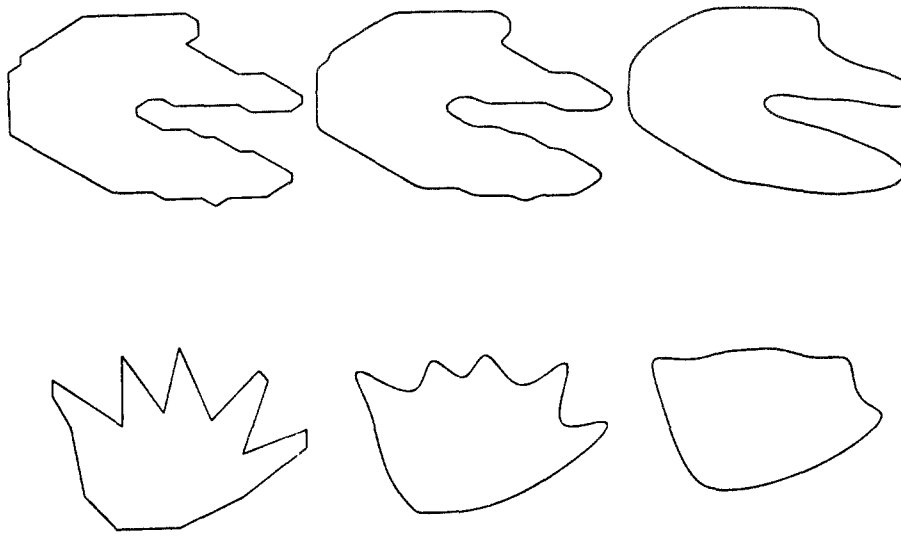

Fig. 4. The smoothing property of the *BAIM* is shown in this example. The curve is getting more and more smooth when the order of the B-spline approximation is increased.

we have that:

$$\begin{aligned} C_k(u) &= \sum_{i=1}^{N} V_i B_{i,k} \\ &= \sum_{i=1}^{N} (x_i + jy_i) \left[\sum_{m=-\infty}^{m=\infty} \exp\{jm\pi i\} \left(\frac{2\sin(m\pi/2)}{m\pi} \right)^k \exp\{jm\pi u\} \right] \\ &= \sum_{m=-\infty}^{m=\infty} \left(\sum_{i=1}^{N} (x_i + jy_i) \exp\{jm\pi i\} \right) \left(\frac{2\sin(m\pi/2)}{m\pi} \right)^k \exp\{jm\pi u\}. \end{aligned}$$

We see that when k increases ($k \to \infty$), the B-spline representation converges to the centroid of the initial polygon (only the term for $m = 0$ remains in the sum). Furthermore, the convergence is in such a way that the curve shape approaches an ellipse. This is so since high frequency components of the Fourier transform of the *BAIM* die out much faster than the low frequency ones. Therefore, the limiting curve becomes approximately an ellipse, when only the zero ($m = 0$) and first ($m = \pm 1$) frequency components remain significant (compare this results with the polygonal ellipse in Theorem 4). □

Figure 4 gives examples showing the smoothing property of the *BAIM*. Actually, it can be proven formally that the *BAIM* is a smoothing process with increasing exponent, i.e., the total difference of any order decreases with k [33, 41]. See [34] for details on the smoothing properties of this representation.

5. Concluding Remarks

In this paper, we presented three different affine invariant smoothing processes for planar curves. The first one is derived from a *geometric heat-type flow*, were both the initial and the smoothed curves are differentiable. This scheme can be extended to non-smooth initial curves based on the results in [4]. The second one is obtained from a discretization of this affine heat equation. In this case the curves are represented by *polygons*. The third process is derived from *B-spline* approximations. For this process, the initial curve is given by a polygon, and the smoothed curves are differentiable and analytic. Then, the processes presented can be described schematically, with respect to the type of curves involved, as differentiable→differentiable, discrete→discrete, and discrete→differentiable (analytic), respectively.

Note also that in the first model, the time scale (smoothing scale), is continuous ($t \in [0, \tau]$). In the second one, this scale is discrete, but c can be taken as small as required, and as c decreases, we approach a continuous time evolution process. In the last model, the smoothing scale is related to the B-spline order, therefore, it is strictly discrete ($k = 2, 3, \ldots$). In the first case we could also propose a 'discrete time' evolution process, where $C(n, p)$ is obtained by averaging over a given constant affine arc length neighborhood of $C(n-1, p)$. This is, for small averaging neighborhoods, an affine invariant numerical approximation of the affine geometric heat flow. To complete the picture, it would be interesting to also find a 'continuous time', B-spline based, smoothing process. This was recently developed in [34] using subdivision schemes.

We showed that the three processes discussed deform any initial curve into an *elliptic point*. This nice result is hardly unexpected, since the processes are affine invariant smoothing operations, and the ellipse is the smoothest affine invariant shape. What is interesting to note is that each type of smoothing process required a different approach to prove the result.

We conclude this paper with an interesting question that arises from the work presented here: Given an initial continuous curve, and a polygon obtained by sampling it, what is the relation between the evolving curve obtained via the affine heat flow (with the continuous curve as initial condition), and the curves obtained with the other smoothing processes (with the polygon as initial condition). This, and the other open questions mentioned above, are subject to further research.

Acknowledgments

We thank Dr Lyle Ramshaw from Digital Systems Research Center for providing us his monograph [32], Prof. Gil Kallai from the Hebrew University for pointing out the old results by Darboux, and Mr Dario Ringach from New York University, who located for us the beautiful paper of Darboux.

References

1. Alvarez, L., Guichard, F, Lions, P. L. and Morel, J. M.: Axiomes et equations fondamentales du traitement d'images, *C.R. Acad. Sci. Paris* **315** (1992), 135–138.
2. Alvarez, L., Guichard, F., Lions, P. L. and Morel, J. M.: Axiomatisation et nouveaux operateurs de la morphologie mathematique, *C.R. Acad. Sci. Paris* **315** (1992), 265–268.
3. Alvarez, L., Lions, P. L. and Morel, J. M.: Image selective smoothing and edge detection by nonlinear diffusion, *SIAM J. Numer. Anal.* **29** (1992), 845–866.

4. Angenent, S., Sapiro, G. and Tannenbaum, A.: On the affine heat flow for non-convex curves, MIT-LIDS Internal, Report, March 1994.
5. Babaud, J., Witkin, A. P., Baudin, M. and Duda, R. O.: Uniqueness of the Gaussian kernel for scale-space filtering, *IEEE Trans. Pattern Anal. Machine Intell.* **8** (1986) 26–33.
6. Bartles, R. H., Beatty, J. C. and Barsky, B. A.: *An Introduction to Splines for Use in Computer Graphics and Geometric Modeling*, Morhan Kaufmann, California, 1987.
7. Berlekamp, E. R., Gilbert, E. N. and Sinden, F. W.: A polygon problem, *Amer. Math. Monthly* **72** (1965), 233–241.
8. Blaschke, W.: *Vorlesungen über Differentialgeometrie II*, Verlag Von Julius Springer, Berlin, 1923.
9. Bourdeau, M. and Dubuc, S.: L'itération de Fejes Tóth sur un polygone, *J. Geom.* **6** (1975), 65–75.
10. Bruckstein, A. M. and Netravali, A. N.: On differential invariants of planar curves and recognizing partially occluded planar shapes, *Proc. Visual Form Workshop*, Capri, May 1991, Plenum Press, New York.
11. Bruckstein, A. M., Sapiro, G. and Shaked, D.: Evolutions of planar polygons, CIS Report 9202, Department of Computer Science, Technion, IIT, Haifa 32000, Israel, 1992, to appear in *Int. J. Patt. Recog. and AI.*
12. Cadwell, J. H.: A property of linear cyclic transformations, *Math. Gazelte* **37** (1953), 85–89.
13. Clarke, R. J.: Sequences of polygons, *Math. Magazine* **52** (1979), 102–105.
14. Davis, P. J.: Cyclic transformations of polygons and the generalized inverse, *Canad J. Math.* **39** (1977), 756–700.
15. Darboux, M. G.: Sur un probleme de geometrie elementaire, *Bull. Sci. Math.* **2** (1878), 298–304.
16. Dieudonné, J. and Carrell, J.: *Invariant Theory: Old and New*, Academic Press, London, 1970.
17. De Boor, C.: *A Practical Guide to Splines*, Applied Mathematical Sciences 27, Springer-Verlag, New York, 1978.
18. De Boor, C.: *Spline Toolbox for use with MATLAB*^{TM}, The Math Works, Inc., Natick, 1990.
19. Fejes Tóth, G.: Iteration processes leading to a regular polygon, *Mat. Lapok* **23** (1970), 135–141, (in Hungarian).
20. Fejes Tóth, L.: Iteration methods for convex polygons, *Mat. Lapok* **20** (1969), 15–23, (in Hungarian).
21. Gage, M. and Hamilton, R. S.: The heat equation shrinking convex plane curves, *J. Differential Geom.* **23** (1986), 69–96.
22. Gonzalez, R. C. and Wintz, P.: *Digital Image Processing*, Addison-Wesley, Reading, Mass, 1987.
23. Grayson, M.: The heat equation shrinks embedded plane curves to round points, *J. Differential Geom.* **26** (1987), 285–314.
24. Hummel, A.: Representations based on zero-crossings in scale-space, *Proc. IEEE Computer Vision Pattern Recog. Conf.*, 1986, pp. 204–209.
25. Kimia, B. B., Tannenbaum, A. and Zucker, S. W.: Toward a computational theory of shape: An overview, *Lecture Notes in Computer Science* 427, Springer-Verlag, New York, 1990, pp. 402–407.
26. Kimia, B. B., Tannenbaum, A. and Zucker, S. W.: Shapes, shocks, and deformations, I, to appear in *Internat. J. Computer Vision.*
27. Koenderink, J. J.: The structure of images, *Biological Cybernetics* **50** (1984), 363–370.
28. Korchmáros, G.: An iteration process leading to affinely regular polygons, *Mat. Lapok.* **20** (1969), 405–401, (in Hungarian).
29. Lükó, G.: Certain sequences of inscribed polygons, *Period. Math. Hungar.* **3** (1973), 255–260.
30. Mokhatarian, F. and Mackworth, A.: A theory of multiscale, curvature-based shape representation for planar curves, *IEEE Trans. Pattern. Anal. Machine Intell.* **14** (1992), 789–805.
31. Osher, S. J. and Sethian, J. A.: Fronts propagation with curvature dependent speed: Algorithms based on Hamilton-Jacobi formalutions, *J. Comput. Phys.* **79** (1988), 12–49.
32. Ramshaw, L.: *Blossoming: A Connect-the-Dots Approach to Splines*, Digital, Systems Research Center, Palo Alto, 1987.
33. Sapiro, G. and Bruckstein, A. M.: A B-spline based affine invariant multiscale shape representation, CIS Report 9303, Department of Computer Science, Technion, IIT, Haifa 32000, Israel, January 1993.
34. Sapiro, G., Cohen, A. and Bruckstein, A. M.: A subdivision scheme for continuous scale B-splines and affine invariant progressive smoothing, MIT-LIDS Internal Report, January 1994.
35. Sapiro, G. and Tannenbaum, A.: On affine plane curve evolution, *J. Funct. Anal.*, **119**(1), January 1994.
36. Sapiro, G. and Tannenbaum, A.: Affine shortening of non-convex plane curves, EE Publication 845, Department of Electrical Engineering, Technion, IIT, Haifa 32000, Israel, July 1992.
37. Sapiro, G. and Tannenbaum, A.: Affine invariant scale-space, *Internat. J. Computer Vision* **11**(1) (1993), 25–44.
38. Sapiro, G. and Tannenbaum, A.: On invariant curve evolution and image analysis, *Indiana Univ. Math. J.* **42**(3) (1993).

39. Schoenberg, I. J.: The finite Fourier series and elementary geometry, *Amer. Math. Monthly* **57** (1950), 390–404.
40. Schoenberg, I. J.: *Cardinal Spline Interpolation*, SIAM Press, Philadelphia, 1973.
41. Schoenberg, I. J.: *Selected Papers II*, edited by C. de Boor, Birkhauser, Boston, 1988.
42. Shapiro, D. B.: A periodicity problem in plane geometry, *Amer. Math. Monthly* **99** (1984), 97–108.
43. Spivak, M.: *A Comprehensive Introduction to Differential Geometry*, Publish or Perish Inc, Berkeley, Calif., 1979.
44. Witkin, A. P.: Scale-space filtering, *Internat. Joint. Conf. Artificial Intelligence*, 1983, pp. 1019–1021.
45. Wong, E. T. H.: Polygons, circulant matrices and Moore-Penrose inverses, *Amer. Math. Monthly* **88** (1981), 509–515.
46. Yuille, A. L. and Poggio, T. A.: Scaling theorems for zero crossings, *IEEE Trans. Pattern Anal. Machine Intell.* **8** (1986), 15–25.